Synthesis of CEG-AgNPs as a Promising MMPs/COX-2/Bcl-2 Signaling Pathway Modulator in BaP-Induced Lung Carcinoma

Ahmed A. Emara[1], Ahmed M. Darwesh[1], Mohamed A. Mostafa[1], Ahmed A. Ahmed[1], Khaled W. Rashad[1],
Abdullah M. Said[1], Abdelrahman E. Elsebaay[1], Khaled M. Nasser[1], Abdelrehem S. Amin[1], Mohamed S. Gamil[1],
Foad H. Mohamed[1], Mohamed K. Ahmed[1], Diana A. Alshrief[1], Mohammed E. Hassan[2],
Zahraa Nassar[2], Amr A. El-Ella[3], Mostafa A. Abdel-Maksoud[4] and Mohammed A. Hussein[5,*,iD]

[1]Department of Radiology and Medical Imaging, Faculty of Applied Medical Science, October 6th University, October 6th City, Egypt
[2]Department of Medical Laboratories, Faculty of Applied Medical Sciences, October 6 University, Sixth of October City, Egypt
[3]Department of Measurements, Photochemistry and Agriculture Applications. National Institute of Laser Enhanced Science, Cairo University, Giza, Egypt
[4]Department of Radiology and Medical Imaging, Faculty of Medicine, Sudan University of Sciences and Technology, Khartoum, Sudan
[5]Department of Biochemistry, Faculty of Applied Medical Science, October 6th University, October 6th City, Egypt

*Corresponding author: Tel: +20 124832580; E-mail: prof.husseinma@o6u.edu.eg

Cucurbitacins are a class of highly oxidized tetracyclic triterpenoids. It's hydrophobic properties and poor solubility in water, polymeric micellar systems exhibited improved antitumor efficacy because of a better solubilization and targeting after local and/or systemic administration. The aim of the present work was to evaluate the anticancer activity of CEG-AgNPs against benzo[a]pyren (BaP)-induced lung carcinoma. CEG-AgNPs was prepared, characterized and evaluated for its cytotoxic activity against A549 lung carcinoma cell line. Also, the anticancer activity of CEG-AgNPs (70.25 mg/kg) against BaP-induced lung carcinoma was evaluated *in vivo*, using 30 adult mice for 43 days. IC_{50} of CEG-AgNPs against A549 lung carcinoma cell line were approximately 94.47 µg/mL. Administration of BaP (50 mg/kg b.w.) to mice induced lung carcinoma with a significant increase in lung MMP-2, MMP-9, MMP-12, MDA, IL-6 and NF-κB as well as significant decreased in lung CAT, GPx and GSH level. Also, treatment with BaP produced significant increase in lung VEGF-C, COX-2 and Bcl-2 gene expression as compared to control group. Daily oral administration of CEG-AgNPs to mice treated with BaP showed a significant protection against-induced increase in lung MMP-2, MMP-9, MMP-12, MDA, IL-6 and NF-κB levels. The treatment also resulted in a significant increase in lung CAT, GPx and GSH level. In addition, the CEG-AgNPs could inhibit lung VEGF-C, COX-2 and Bcl-2 gene expression as compared to BaP treated mice. The histological and MRI examination showed that a significant normalization has been observed through in CEG-AgNPs treated mice. The biochemical, histological and MRI results showed that CEG-AgNPs have potent anticancer activity against BaP-induced lung carcinoma through modulating multiple cellular behaviours and signaling pathways leading to the suppression of adaptive immune responses.

Keywords: Cucurbitacin-E-glucoside, BaP, Lung carcinoma, Gene expression, Antioxidant enzyme, Cytokine storm.

INTRODUCTION

Cancer is an uncontrolled division of cells that results in the death of abnormal tissue. In both men and women worldwide, lung cancer is believed to be the leading cause of mortality [1,2]. Some 85% of the lung smoking is responsible for cancer [3,4]. Polycyclic aromatic hydrocarbon (PAHs), the main component of smoke, such as benzo[a]pyren (BaP) [5].

Long-term exposure to low levels of some PAHs have caused cancer in laboratory animals [6]. Benzo[a]pyrene is the most common PAH to cause cancer in animals [7]. Several studies reported that workers exposed to mixtures of PAHs and other compounds have noted an increased risk of skin, lung, bladder and gastrointestinal cancers [8]. It can diffuse into cells and binds to aryl hydrocarbon receptor [9]. Upon binding, it translocates into the nucleus and binds to xenobiotic response

elements of target genes [10]. This results in the transcription of genes that encode for enzymes involved in xenobiotic detoxification, including CYP1A1 and CYP1B1 [11]. The detoxification of BaP is a multistep process involving a number of critical enzymes. The first stage requires an epoxidation reaction by the mono-oxygenases CYP1A1 and CYP1B1 (phase I) that requires NADPH and molecular oxygen. One of the resulting metabolites (*e.g.* BaP-7,8-epoxide) can be converted to a dihydrodiol (*e.g.* BaP-7,8-dihydrodiol) by epoxide hydrolase. BaP-7,8-dihydrodiols can be further metabolized by CYP1A1 or CYP1B1 to diol epoxides (*e.g.* BaP-7,8-diol-9,10-epoxide, BPDE) or conjugated by uridine diphosphate glucuronosyl transferase (UGT) (phase II) [12]. BPDE is the active mutagenic compound as it can covalently bind to DNA to form premutagenic adducts [11].

Triterpenes are a major class of plant, fungal and animal natural products. In addition, triterpenoids exhibit a range of biological functions, including antimicrobial, antitumor, anti-inflammatory, antiviral and antioxidant activities [13]. It is therefore not surprising that cucurbitacins found in medicinal plants, are used for cancer treatment. Cucurbitacin E has been shown to have remarkable suppressing the proliferation of multiple cancer cell types, such as lung cancer, breast cancer, neuroblastoma, endometrial cancer and hepatocellular carcinoma [14-16]. Also, it suppresses cytokine expression by inhibiting the activation of NF-κB [17] and inhibits of Wnt/β-catenin signaling [18].

Silver nanoparticle (AgNP) is among the most effective metallic nanoparticles of combating bacteria and viruses [19]. Furthermore, the resistance to silver is unlikely to develop, as the metal attacks a wide range of target sites in the organisms [20]. The proposed mechanism of formation of AgNPs using plant phytochemicals can proceed through three steps [21]: first, charge transfer from reducing agents to Ag^+ results in the formation of Ag atoms, which subsequently nucleate to form small AgNPs; second, a condensation step occurs in which small particles grow to form larger ones, followed by surface reduction of any Ag^+ present on the surface of the formed NPs; and third, adsorption of excess negatively charged reducing agents ions on the surface of the formed particles, achieving electrostatic stabilization and thus controlling their sizes [22].

To our knowledge, there are no studies have been reported the efficacy of cucurbitacin E glucoside nanoparticles for the suppression of lung cancer growth. As a continuation of our ongoing investigation in the therapeutic potential of natural products nanoparticles [23,24]. A simple method for evaluating the anticancer activity of CEG-AgNPs against benzo[a]pyren (BaP)-induced lung carcinoma in mice is reported.

EXPERIMENTAL

The current study was carried out at the Faculty of Applied Medical Sciences, October 6 University, Egypt during August, 2020. Cucurbitacin-E-glucoside (95%) and benzo[a]pyren (BaP) were purchased from Sigma Chemical Co., St Louis, USA. All other chemicals used were of analytical grade.

Synthesis of CEG-AgNPs: A 1 mM aqueous solution of silver nitrate ($AgNO_3$) was prepared. Cucurbitacin-E-glucoside (300 mg) was dissolved in little amount of ethanol and volume makeup to 100 mL by distilled water. To a 60 mL of cucurbitacin-E-glucoside solution, added 10 mL of $AgNO_3$ solution, with continuous stirring and heating at 60 ºC for 10 h; after which 200 mL of 40 mM ascorbic acid was added as a catalyst and the brown CEG-AgNPs were suspended and characterized by TEM technique [25].

CEG-AgNPs characterization: The X-ray diffraction pattern of CEG-AgNPs was determined at 25-28 ºC with nickel (Ni) (D8 advance X-ray diffractometer) filtered using Cu$K\alpha$ ($\lambda = 1.54184$ Å) radiation as X-rayed source. The morphology and size of the CEG-AgNPs were studied using a scanning electron microscope and a field transmission microscope at accelerating voltages of 15 kV and 200 kV, respectively.

Determination of CEG-AgNPs cytotoxicity on lung carcinoma A549 cell line: Assessment of relative numbers of viable cells will be done using MTT tetrazolium assay (SERVA, Germany). Briefly, all cells were seeded in 96-well plate at density of 1.0×10^6 cells/well for 24 h incubation at standard conditions. After 1 day, CEG-AgNPs was evaluated in this assay in triplicates at six doses concentration (31.5, 62.5, 125, 250, 500 and 1000 µg/mL) for 24 h. A MTT reagent (10 µL) in fresh media (5 µg/mL) was added to each well. The reaction was stopped after 4 h incubation by adding 100 µL of DMSO for 20 min at 37 ºC to form violet formazan crystals and the optical density was measured at 550 nm with a microplate reader (800TSUV Biotek ELISA Reader). Negative control cells are those treated with 0.1% DMSO solvent vehicle only.

Animals: Adult albino mice weighing approximately 35 ± 4 g were obtained from Cairo University's animal house in Giza, Egypt. The animals were kept in a light-controlled room at 22 ºC and a humidity of 55-60%. The animals were kept for a week to acclimate before being fed a standard diet and given unlimited water.

Experimental setup: This experiment was carried out to examine the protective effect of CEG-AgNPs against B[a]P-induced lung carcinoma. This experiment was conducted in accordance with guidelines established by the Animal Care and Use Committee of October 6th University. Adult albino mice were divided into five groups with six animals in each. The treatment groups are described in Table-1.

At day 43, *i.e.* one day after the last treatment, cervical decapitation sacrificed mice from each group. The lung specimens were quickly retrieved and gently opened with a scrapper, rinsed using ice-cold isotonic saline to remove all blood cell types and clots, then blotted between 2 filter documents and divided one part 3 parts.

The first part was homogenized with ice-cold saline in a glass homogenizer (Universal Lab. Aid MPW-309, Poland) to make a 25% w/v homogenate. The homogenate was prepared in four aliquots. The first aliquot was used to evaluate the metalloproteinases (MMPs) activity. The MMP-2 was quantified in lung tissues by its catalytic effect on the *N*-succinyl-trialanyl-*p*-nitroanilide substrate as described by Mahor *et al.* [26]. MMP-12 enzymatic activity was quantified in lung tissue by using the gelatin zymography [23]. The second aliquot was deproteinized with 12% (ice-cold trichloroacetic acid), centri-

TABLE-1
DESCRIPTION OF TREATMENT GROUPS

Group	Group name	Treatment description
I	Normal control A	3 mL of distilled water orally for 30 days
II	CEG-AgNPs	Mice treated with 70.25 mg/kg b.w. CEG-AgNPs in DMSO from week 1 to week 6.
III	BaP	Mice treated with 50 mg/kg of BaP dissolved in sesame oil by oral gavages from week 1 to week 3.
IV	BaP + CEG-AgNPs (treatment)	Mice treated with 50 mg/kg of BaP dissolved in sesame oil by oral gavages from week 1 to week 3 and later treated with 70.25 mg/kg b.w. CEG-AgNPs in DMSO + 50 mg/kg of BaP from week 4 to week 6.
V	CEG-AgNPs + BaP (prophylactic)	Mice treated with 70.25 mg/kg b.w. CEG-AgNPs in DMSO +50 mg/kg of BaP from week 1 to week 3 and later treated with 70.25 mg/kg b.w. CEG-AgNPs in DMSO from week 4 to week 6.

fuged at 1000 xg and obtained supernatant was used to calculate GSH.

The supernatant from the third aliquot was used to calculate the levels of malondialdehyde (MDA), interleukin 6 (IL-6) and nuclear factor kappa (NF-κB). The fourth aliquot of homogenate was used to prepare a cytosolic fraction of the mammary by centrifuging it at 10500 xg for 15 min at 4 ºC in a cooling ultra-centrifuge (Sorvallcomiplus T-880, Du Pont, USA) and the clear supernatant (cytosolic fraction) was used to determine the activities of CAT and GPx using rat ELISA kit, which is an *in vitro* enzyme (ELISA). The test was carried out in accordance with the supplier's protocol (Rapid, Bio. Laboratories, Inc.).

Quantitative real-time PCR: The total RNA extracted was extracted from the second part of lung. The portions of (10-15 µg) of the isolated RNA were subjected to quantitative PCR analysis in real time, using Sepasol-RNA1 super according to instructions of the manufacturer. The two-step RT-PCR gene expression has been measured. The level of VEGF-C, COX-2 and Bcl2 were quantified with the previously described quantitative real-time PCR. The tests in 50 mL single-plex reaction mixture were conducted. Conditions of reaction were a pre-incubation at 50 ºC in 2 min, followed by 10 min by 40 cycles of 95 ºC in 15 s and 60 ºC in 1 min, respectively.

The primer sequences were VEGF-C: F 52-AACGTGTCCAAGAAATCAGCC-32, R: 52-AGTCCTCTCCCGCAGTAATCC-32. COX-2: Forward: CTG TAT CCC GCC CTG CTG GTG. Reverse: ACT TGC GTT GAT GGT GGC TGT CTT. Bcl2: Forward: CTC AGT CAT CCA CAG GGC GA. Reverse: AGA GGG GCT ACG AGT GGG AT. The internal control used GAPDH -F: 52-CTCAACTACATGGTCTACATGTTCCA-32 and -R: 52-CCATTCTCGGCCTTGA-CTGT-3'.

Histological assessment: For histological examination, the third part of lung was cut into pieces and fixed in a 10% buffered formalin solution. The fixed tissues were processed with an automated tissue processing machine. Standard techniques were used to embed tissues in paraffin wax. Kim *et al.* [27] method was used to prepare 5 mL thick sections that were stained with hematoxylin and eosin for light microscopy analysis. The sections were then examined under a microscope for histopathological changes and photomicrographs were taken.

MRI protocol: Once placed on the handling platform, each mouse was fixed in a supine recumbence position and then introduced into the RF coil inside the MRI gantry. Many images and sequences are taken for 3 mice/group to evaluate and compare the results, including CORONAL T1, T2, SAGITAL T1, T2 and STAIR.

Statistical analysis: The results were expressed as mean ± SD for each of the eight separate determinations. All the data was statistically analyzed using SPSS/18 software [28]. To test hypotheses, one-way analysis of variance was used, followed by the least significant difference test ($p \leq 0.05$).

RESULTS AND DISCUSSION

In the current experiments, we explored the possibility that the ability of CEG-AgNPs to protect against carcinogenesis by B[a]P. TEM analysis shows that CEG-AgNPs had size of around 42.32 ± 9.52 nm with negative zeta potential of -17.44 (Fig. 1). The results are reported in Table-2 shows that the incubation of CEG-AgNPs at different consternations (31.25, 62.50, 125, 250, 500 and 1000 µg mL^{-1}) with lung cancer cell lines (A549) resulted in viability% of 98.23, 71.47, 28.13, 9.31, 5.39 and 5.09, respectively and toxicity% of 1.76, 28.52, 71.86, 90.68, 94.60 and 94.90, respectively. The IC$_{50}$ value of CEG-AgNPs against A549 lung carcinoma cells was 94.47 µg mL^{-1}.

Cucurbitacin E glycoside usually has the saccharide linked to carbon atom 2 (2-O-β-glycoside). Cucurbitacins E formed

TABLE-2
DETERMINATION OF CEG-AgNPs TOXICITY ON A549 LUNG CARCINOMA CELL LINE (MTT PROTOCOL)

| Conc. (µg/mL)	Optical density			Mean optical density	Standard error	Viability (%)	Toxicity (%)	IC$_{50}$
DMSO (0.1%)	0.326	0.353	0.341	0.340000	0.007810	100	0	–
1000	0.017	0.018	0.017	0.017333	0.000333	5.098039216	94.90196078	
500	0.018	0.019	0.018	0.018333	0.000333	5.392156863	94.60784314	
250	0.020	0.038	0.037	0.031667	0.005840	9.313725490	90.68627451	94.47
125	0.089	0.105	0.093	0.095667	0.004807	28.13725490	71.86274510	
62.5	0.239	0.236	0.254	0.243000	0.005568	71.47058824	28.52941176	
31.25	0.333	0.326	0.343	0.334000	0.004933	98.23529412	1.764705882	
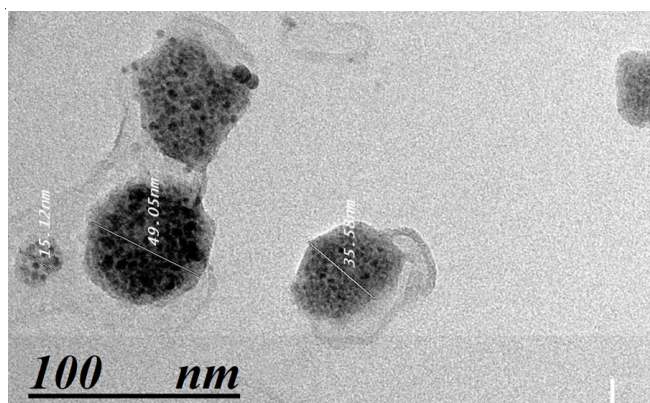
Fig. 1. TEM image (x200) of CEG-AgNPs nanoparticles with a mean size of 42.32 ± 9.52 nm. The CEG-AgNPs nanoparticles exhibit spherical shape and smooth surfaces

from the acetylation of cucurbitacins I, a feature that increased hydrophobicity and cytotoxicity [29]. Nano-sized enhanced the surface area of nanoparticles may show the high bio-adhesion to the gastrointestinal wall, ensuring the higher, effective and prolonged uptake CEG-AgNPs is expected to be protected against carcinogenesis and lung tissue degradation. Also, binding of B[a]P metabolites to DNA and formation of bulky adducts in DNA is the major mechanism of B[a]P-induced mutagenesis and carcinogenesis [30]. To be converted to a carcinogen, B[a]P first needs to be metabolized to its activated metabolites by cytochrome P450 enzymes, that are principally involved in B[a]P activation [31].

In present study, there was significant increase in the lung matrix metalloproteinases levels observed in the BaP treated group as compared with the control group. Table-3 showed the levels of lung MMP-2, MMP-9 and MMP-12 in different groups of mice. There was no difference observed in the levels of lung MMP-2, MMP-9 and MMP-12 in normal mice treated with CEG-AgNPs (70.25 mg/kg b.w.) compared to compared to the normal control group. Also, lung levels of MMP-2, MMP-9 and MMP-12 increased significantly ($p < 0.05$) in B[a]P treated mice by 260.45%, 96.82% and 111.53%, respectively, as compared to control group ($p < 0.05$).

Lung level of MMP-2, MMP-9 and MMP-12 ($p < 0.05$) were significantly decreased by 52.00%, 24.46% and 37.69%, respectively in mice post-treated with CEG-AgNPs (70.25 mg/kg b.w.), as compared to B[a]P treated group. A significant decrease in lung level of MMP-2, MMP-9 and MMP-12 ($p < 0.05$) were observed in the group of mice pre-treated with CEG-

AgNPs (70.25 mg/kg b.w.) by 70.43%, 39.53% and 47.78%, respectively as compared to B[a]P treated group.

Numerous studies have shown that MMP-9 expression is correlated with tumour development and progression and is an important regulator of angiogenesis by releasing VEGF and promoting vascular pericyte recruitment [32]. Immunohisto-chemical analysis of breast tumour tissue revealed a significant association between a strong expression of pro- and active MMP9 in breast tumour tissue and a shortened relapse-free survival, and one study reported this relation in particular in oestrogen positive tissue [33]. Further a relationship between MMP-9 overexpression and a prolonged overall and relapse-free survival in early breast cancer has been demonstrated, although this finding is debatable as only the expression of the inactive proform of MMP-9 was assessed [34,35]. Present results were in confirmation with the data reported by Kamaraj *et al.* [28], who showed that the expressions of matrix metallo-proteinases (MMPs) during benzo[a]pyrene induced lung carcinogenesis in mice.

In present study, the significant increase in lung IL-6 and NF-κB with the concomitant decrease in CAT, GPx and GSH activity were detected after EE-administration. Table-4 shows that significantly increased ($p < 0.05$) in lung MDA, IL-6 and NF-κB levels in B[a]P-treated group by 126.27%, 85.99% and 99.46%, respectively as compared to normal control group. There was no difference observed in the levels of lung MDA, IL-6 and NF-κB in normal mice treated with CEG-AgNPs (70.25 mg/kg b.w.) compared to compared to the normal control group.

A significant decrease in lung MDA, IL-6 and NF-κB levels ($p < 0.05$) were observed in the group of mice post-treated with CEG-AgNPs (70.25 mg/kg b.w.) by 50.80%, 17.05% and 34.34%, respectively as compared to B[a]P-treated group. In the group of mice pre-treated with CEG-AgNPs (70.25 mg/kg b.w.) both MDA, IL-6 and NF-κB levels decreased significantly ($p < 0.05$) by 54.34%, 38.17% and 37.39%, respectively as compared to B[a]P-treated group. The effect was more pronounced in case of pre-administration of CEG-AgNPs (70.25 mg/kg b.w.) before B[a]P injection (group 5) compared to administration of CEG-AgNPs after B[a]P treatment (group 4). Present results is in confirmation with the data published by Majumder *et al.* [36], who reported that BaP induce the expression of various pro-inflammatory cyto-kines and matrix remodelling proteins. It is also responsible for dysfunction and exhaustion of the killing capacity of CD8+ T lymphocytes, one of the important components of the immune

TABLE-3
EFFECT OF CEG-AgNPs ON LEVELS OF ON LUNG MATRIX METALLOPROTEINASES
(MMPs) (MMP-2, MMP-9 AND MMP-12) IN CONTROL AND TREATED MICE

Groups	Treatment description	MMP-2 (U/g tissue)	MMP-9 (U/g tissue)	MMP-12 (U/g tissue)
I	Normal control	42.66 ± 3.87[a]	18.57 ± 1.25[a]	13.96 ± 1.63[a]
II	CEG-AgNPs (72.25 mg/kg b.w.)	41.50 ± 4.07[a]	18.66 ± 2.77[a]	14.00 ± 1.65[a]
III	BaP (50 mg/kg b.w.)	154.87 ± 9.06[c]	36.55 ± 3.62[c]	29.53 ± 2.60[c]
IV	BaP (50 mg/kg b.w.) + CEG-AgNPs (72.25 mg/kg b.w.) (treatment)	74.33 ± 5.7[b]	27.61 ± 2.15[b]	18.40 ± 1.05[b]
V	CEG-AgNPs (72.25 mg/kg b.w.) + BaP (50 mg/kg b.w.) (prophylactic)	45.80 ± 3.69[a]	22.10 ± 2.69[a]	15.42 ± 2.25[a]

Data shown are mean ± standard deviation of number of observations within each treatment. Data followed by the same letter are not significantly different at $p \leq 0.05$.

TABLE-4
EFFECT OF CEG-AgNPs ON LEVELS OF LUNG MALONDIALDEHYDE (MDA), INTERLEUKIN 6
(IL-6) AND NUCLEAR FACTOR KAPPA (NF-κB) IN CONTROL AND TREATED MICE

Groups	Treatment description	MDA (nmol/mg tissue)	IL-6 (pg/mg tissue)	NF-κB (ng/g tissue)
I	Normal control	174.76 ± 10.38[a]	235.87 ± 21.74[a]	546.70 ± 17.25[a]
II	CEG-AgNPs (72.25 mg/kg b.w.)	173.25 ± 14.65[a]	232.98 ± 17.68[a]	535.80 ± 26.48[a]
III	BaP (50 mg/kg b.w.)	395.43 ± 25.76[d]	438.70 ± 30.65[c]	1090.37 ± 24.75[d]
IV	BaP (50 mg/kg b.w.) + CEG-AgNPs (72.25 mg/kg b.w.) (treatment)	194.55 ± 15.84[c]	363.89 ± 20.87[b]	715.90 ± 32.48[c]
V	CEG-AgNPs (72.25 mg/kg b.w.) + BaP (50 mg/kg b.w.) (prophylactic)	180.54 ± 19.00[b]	271.25 ± 16.33[a]	682.66 ± 21.75[b]

Data shown are mean ± standard deviation of number of observations within each treatment. Data followed by the same letter are not significantly different at $p \leq 0.05$.

system which can kill tumor cells. An additional metabolic pathway identified in lung but not liver microsomes, is auto-oxidation of B[a]P radical cation metabolites resulting in formation of quinones [37]. As well as being electrophiles that form DNA adducts, the B[a]P quinones may undergo redox-cycling which ultimately results in production of superoxide and other ROS [38,39].

Table-5 showed non-significant changed in lung CAT, GPx and GSH levels of normal mice treated with CEG-AgNPs (70.25 mg/kg b.w.) as compared to the control group. Also, the obtained data shows a significant decrease in levels of lung CAT, GPx and GSH ($p < 0.05$) in mice treated with B[a]P (50 mg/kg b.w.) by 63.21%, 57.28% and 62.83%, respectively, as compared to the control group. The post-treatment of CEG-AgNPs (70.25 mg/kg b.w.) showed significant increase in GPx, CAT and GSH by 110.57%, 113.27% and 101.21%, respectively compared with the B[a]P (50 mg/kg b.w.) treated group of mice ($p < 0.05$). Also, pre-treatment of CEG-AgNPs (70.25 mg/kg b.w.) showed significant increase in GPx, CAT and GSH by 145.40%, 126.11% and 159.40%, respectively compared with the B[a]P (50 mg/kg b.w.) treated group of mice ($p < 0.05$).

As an indicator of lung carcinosis and oxidative stress; inflammatory markers (VEGF-C, COX-2 and Bcl-2) was measured in the lung. The lung VEGF-C, COX-2 and Bcl-2 gene expression, increased significantly in the BaP-treated rats, while post- or pre-treatment of CEG-AgNPs prevented VEGF-C, COX-2 and Bcl-2 gene expression induced by BaP. Figs. 2-4 display that B[a]P (50 mg/kg b.w.) promoted the VEGF-C, COX-2 and Bcl-2 gene expression in mammary tissues of B[a]P-treated mice compared with control group. Administration of CEG-AgNPs (70.25 mg/kg b.w.) significantly ($p < 0.05$, led to a statistically significant decrease of VEGF-C, COX-2 and Bcl-2 gene expression relative to B[a]P treated group of mice ($p < 0.05$).
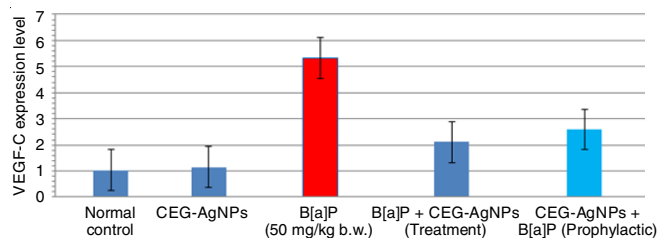

Fig. 2. Effect of CEG-AgNPs (70.25 mg/kg b.w.) on levels of lung vascular endothelial growth factor C (VEGF-C) gene expression in BaP-treated mice. Representative bar diagram of three independent experiments is presented
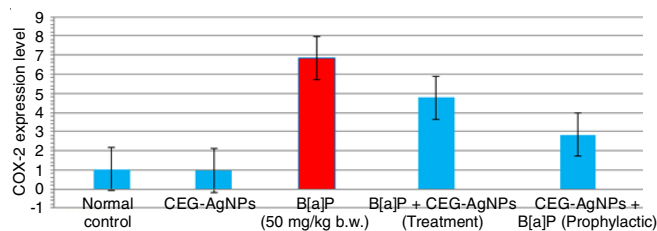

Fig. 3. Effect of CEG-AgNPs (70.25 mg/kg b.w.) on levels of lung cyclooxygenase-2 (COX-2) gene expression in BaP-treated mice. Representative bar diagram of three independent experiments is presented
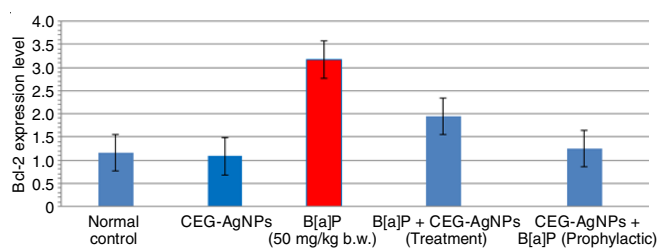

Fig. 4. Effect of CEG-AgNPs (70.25 mg/kg b.w.) on levels of lung B-cell lymphoma 2 (Bcl-2) gene expression in BaP-treated mice. Representative bar diagram of three independent experiments is presented

TABLE-5
EFFECT OF CEG-AgNPs ON LEVELS OF LUNG CATALASE (CAT) AND GLUTATHIONE
PEROXIDASE (GPx) AND REDUCED GLUTATHIONE (GSH) IN CONTROL AND TREATED MICE

Groups	Treatment description	CAT (U/g tissue)	GPx (U/g tissue)	GSH (mg/g tissue)
I	Normal control	13.89 ± 0.87[c]	64.38 ± 5.10[c]	97.33 ± 5.55[c]
V	CEG-AgNPs (72.25 mg/kg b.w.)	12.54 ± 0.96[c]	62.18 ± 3.83[c]	96.45 ± 3.08[c]
III	BaP (50 mg/kg b.w.)	5.11 ± 0.38[a]	27.50 ± 3.94[a]	36.18 ± 3.09[a]
IV	BaP (50 mg/kg b.w.) + CEG-AgNPs (72.25 mg/kg b.w.) (treatment)	10.76 ± 0.84[b]	58.65 ± 4.00[b]	72.80 ± 4.18[b]
V	CEG-AgNPs (72.25 mg/kg b.w.) + BaP (50 mg/kg b.w.) (prophylactic)	12.54 ± 0.96[c]	62.18 ± 3.83[c]	93.85 ± 4.64[c]

Values are given as mean ± SD for groups of six animals each. Values Data followed by the same letter are not significantly different at $p \leq 0.05$.

The present data proved that the pre-treatment of B[a]P-injected mice with CEG-AgNPs produce an inflammatory mediator's suppressive effect more pronounced than post-treatment and no significant chance in normal mice when treated with CEG-AgNPs (70.25 mg/kg b.w.) and compared to normal control group of mice. In support of this, CEG-AgNPs significantly decreased the mRNA levels of VEGF-C, COX-2 and Bcl-2, three target genes of NF-κB, in lung carcinoma. In addition, CEG-AgNPs downregulated IL-6 and matrix metallo-proteinases and increased the cell apoptosis. Collectively, these results suggest that CEG-AgNPs exhibits its anti-inflammatory activity through modulating multiple cellular behaviours and signaling pathways, leading to the suppression of the adaptive immune response [40,41].

According to histological and MRI studies, CEG-AgNPs have a lung protective effect. Histopathological examination of lung sections of the normal group (I) showed within normal apparency x 400 H&E (Fig. 5a). No histopathological changes in normal group of mice by administration with CEG-AgNPs (70.25 mg/kg b.w.) only, (Groups 5b). On the other hand, in the lung tissue of B[a]P-treated control group (III), histological examination showed collapsed alveoli (the black arrow), with many lymphocytic aggregates, hemorrhage and tumorous growth was found in both fibrous tissue and mammary gland X200H&E (Fig. 5c). Histopathological examination also

showed moderate recovery of B[a]P-induced lung injury by post-treatment of CEG-AgNPs (70.25 mg/kg b.w.) as compared to the B[a]P-treated mice (Groups 5d). In Fig. 5e, shows showed patent alveoli, with minimal lymphocytic collections in lung tissue by oral pre-treatment of CEG-AgNPs (70.25 mg/kg b.w.) to B[a]P-treated mice. Because lung proliferation is an early event in damage-related changes, the attenuation of lung injury and fibrosis in mice by CEG-AgNPs could be associated with a reduction in inflammatory response.

MRI examination of lung tissues of the normal group (I) shows normal architecture of lung tissue (Fig. 6a). No lung lesions or inflammation in mice treated with CEG-AgNPs (70.25 mg/kg b.w.) only, Fig. 6b. Also, the lung MRI examination of B[a]P -treated mice (III), show inflammatory lung tissue, hence suggestive of mixed lung tumour (Fig. 6c).

MRI examination also showed moderately improvement in B[a]P-treated mice post-treated with CEG-AgNPs (70.25 mg/kg b.w.) as compared with the B[a]P -treated mice (IV) (Fig. 6d). In addition, lung examination by MRI from B[a]P-treated mice pre-treated with CEG-AgNPs (70.25 mg/kg b.w.) group (V) showed lung tissue improvement (Fig. 6e).

Conclusion

The present results showed that CEG-AgNPs inhibited the proliferation and proinflammatory cytokine expression in
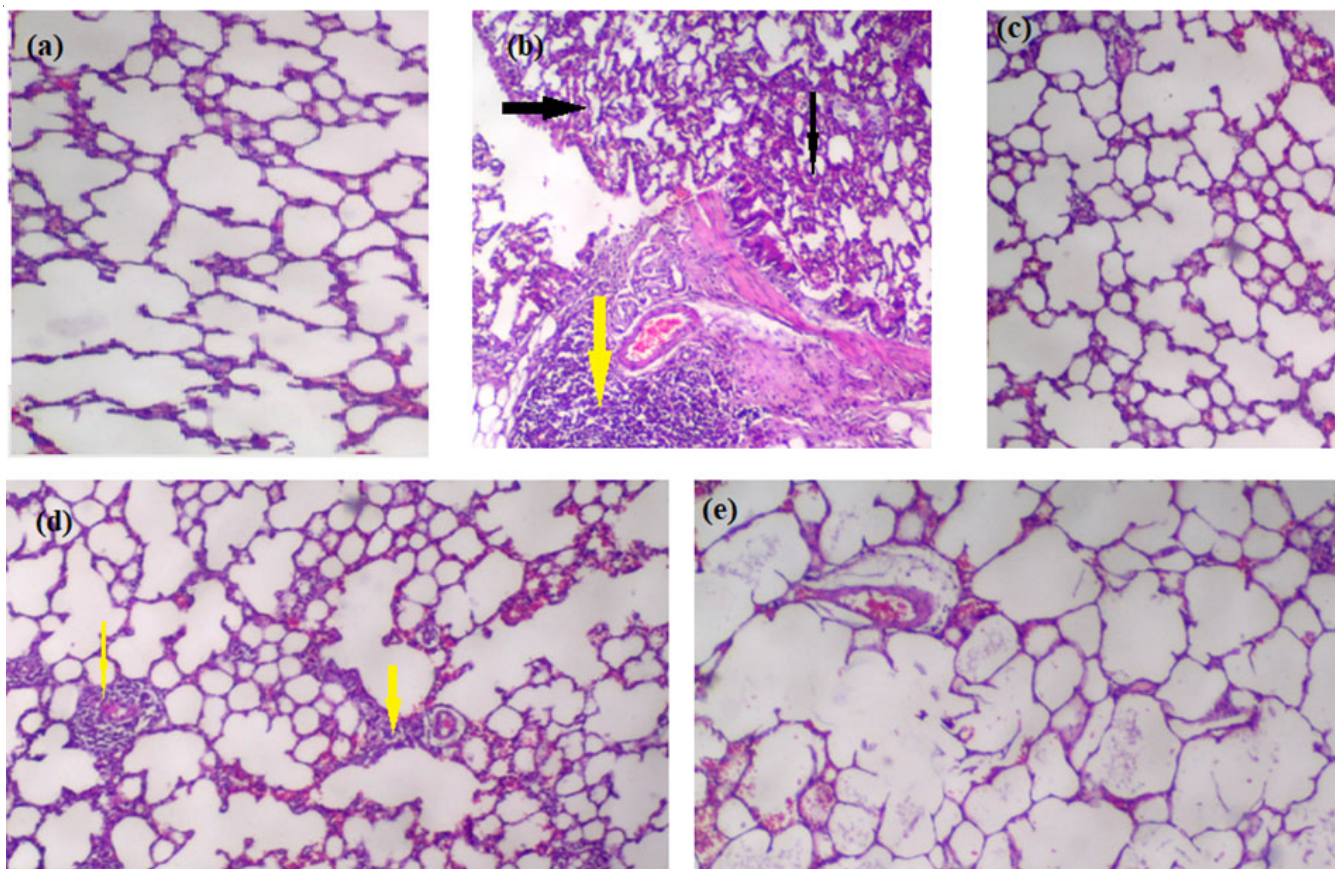

Fig. 5. Sections stained with hematoxylin and eosin (H&E; 400 X) histological examination of mice' lung tissues of different groups compared to control group; (a), Group I: Normal control; (b), Group II: Was administrate CEG-AgNPs (72.25 mg/kg b.w.). (c), Group III: BaP (50 mg/kg b.w.) (d); Group IV: Was administrate BaP (50 mg/kg b.w.) + CEG-AgNPs (72.25 mg/kg b.w.) (treatment); (e), Group V: Was administrate CEG-AgNPs (72.25 mg/kg b.w.) + BaP (50 mg/kg b.w.) (prophylactic)
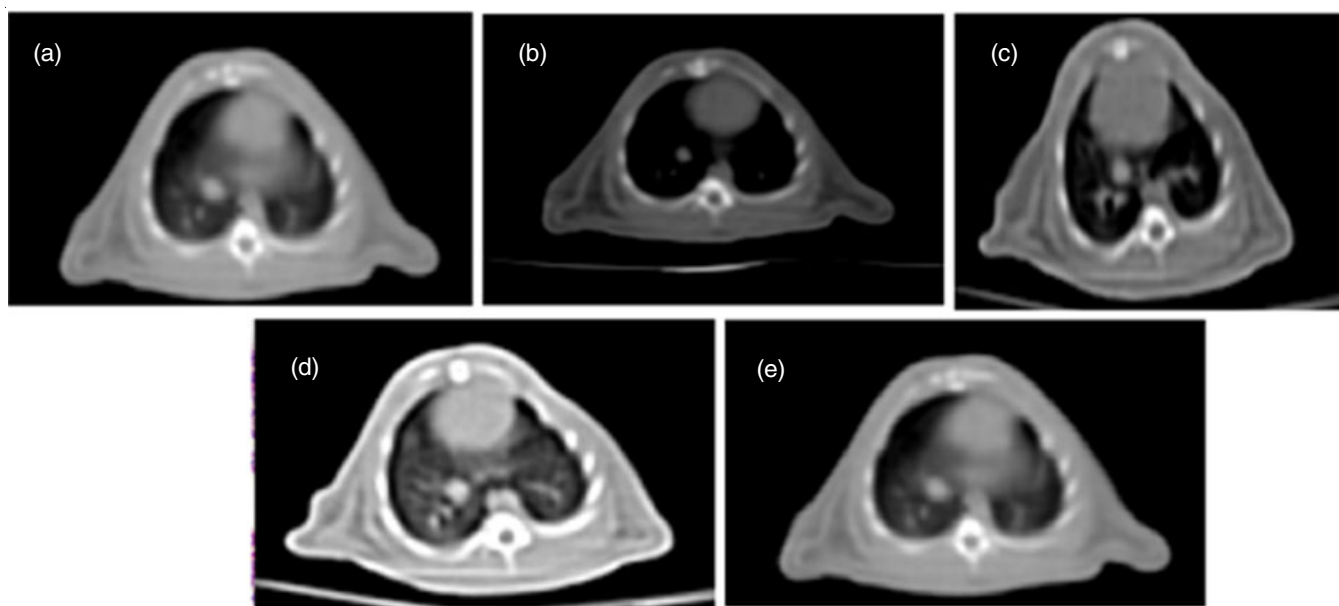
Fig. 6. Magnetic resonance imaging (MRI) examination of mice' lung tissues of different groups compared to control group; (a), Group I: Normal control; (b), Group II: Was administrate CEG-AgNPs (72.25 mg/kg b.w.). (c), Group III: BaP (50 mg/kg b.w.) (d); Group IV: Was administrate BaP (50 mg/kg b.w.) + CEG-AgNPs (72.25 mg/kg b.w.) (treatment); (e), Group V: Was administrate CEG-AgNPs (72.25 mg/kg b.w.) + BaP (50 mg/kg b.w.) (prophylactic)

lung carcinoma. Such inhibitory effects of CEG-AgNPs were probably mediated by blocking nuclear translocation of VEGF-C, COX-2 & Bcl-2 and downregulating NF-κB, IL-6 & matrix metalloproteinases in BaP-induced lung carcinoma. Our data suggest that CEG-AgNPs exhibits its therapeutic activity in inflammation-related diseases through modulating multiple cellular behaviours and signaling pathways leading to the suppression of adaptive immune responses.

CONFLICT OF INTEREST

The authors declare that there is no conflict of interests regarding the publication of this article.

REFERENCES

1. W.J. Scott, J. Howington, S. Feigenberg, B. Movsas and K. Pisters, *Chest*, **132**, 234S (2007);
    https://doi.org/10.1378/chest.07-1378
2. E. Teh, U. Abah, D. Church, W. Saka, D. Talbot, E. Belcher and E. Black, *Interact. Cardiovasc. Thorac. Surg.*, **19**, 656 (2014);
    https://doi.org/10.1093/icvts/ivu206
3. M.A.Hussein, H.A. El-Gizawy, N.A. Gobba and Y.O. Mosaad, *Curr. Pharm. Biotechnol.*, **18**, 677 (2017):
    https://doi.org/10.2174/1389201018666171004144615
4. J.P. Vandenbroucke, *Int. J. Epidemiol.*, **38**, 1193 (2009);
    https://doi.org/10.1093/ije/dyp292
5. R.K. Sticha, E.M. Staretz, M. Wang, H. Liang, M.J. Kenney and S.S. Hecht, *Carcinogenesis*, **21**, 1711 (2000);
    https://doi.org/10.1093/carcin/21.9.1711
6. P. Arulazhagan, K. Al-Shekri, Q. Huda, J.J. Godon, J.M. Basahi and D. Jeyakumar, *Extremophiles*, **21**, 163 (2017);
    https://doi.org/10.1007/s00792-016-0892-0
7. P. Rajendran, T. Jayakumar, I. Nishigaki, G. Ekambaram, Y. Nishigaki, J. Vetriselvi and D. Sakthisekaran, *Int. J. Biomed. Sci.*, **9**, 68 (2013).
8. H.A. Elgizawy, A.A. Ali and M.A. Hussein, *J. Med. Food*, **24**, 89 (2021);
    https://doi.org/10.1089/jmf.2019.0286
9. H.A. El Gizawy, M.A. Hussein and E. Abdel-Sattar, *Pharm. Biol.*, **57**, 485 (2019);
    https://doi.org/10.1080/13880209.2019.1643378
10. A. Amobi-McCloud, R. Muthuswamy, S. Battaglia, H. Yu, T. Liu, J. Wang, V. Putluri, P.K. Singh, F. Qian, R.Y. Huang, N. Putluri, T. Tsuji, A.A. Lugade, S. Liu and K. Odunsi, *Front. Immunol.*, **12**, 678999 (2021);
    https://doi.org/10.3389/fimmu.2021.678999
11. B.J. Moyer, I.Y. Rojas, J.S. Kerley-Hamilton, H.F. Hazlett, K.V. Nemani, H.W. Trask, R.J. West, L.E. Lupien, A.J. Collins, C.S. Ringelberg, B. Gimi, W.B. Kinlaw III and C.R. Tomlinson, *Toxicol. Appl. Pharmacol.*, **300**, 13 (2016);
    https://doi.org/10.1016/j.taap.2016.03.011
12. B.W. Labadie, R. Bao and J.J. Luke, *Clin. Cancer Res.*, **25**, 1462 (2019);
    https://doi.org/10.1158/1078-0432.CCR-18-2882
13. Y.O. Mosaad, N.A. El Khalik Gobba and M.A. Hussein, *Curr. Pharm. Biotechnol.*, **17**, 1189 (2016);
    https://doi.org/10.2174/1389201017666160922110740
14. Y. Kong, J. Chen, Z. Zhou, H. Xia, M.-H. Qiu and C. Chen, *PLoS One*, **9**, e103760 (2014);
    https://doi.org/10.1371/journal.pone.0103760
15. M. Zhang, C. Sun, X. Shan, X. Yang, J. Li-Ling and Y. Deng, *Pancreas*, **39**, 923 (2010);
    https://doi.org/10.1097/MPA.0b013e3181ce719e
16. Q. Zheng, Y. Liu, W. Liu, F. Ma, Y. Zhou, M. Chen, J. Chang, Y. Wang, G. Yang and G. He, *Mol. Med. Rep.*, **10**, 89 (2014);
    https://doi.org/10.3892/mmr.2014.2175
17. H. Feng, L. Zang, Z.X. Zhao and Q.C. Kan, *Cancer Biother. Radiopharm.*, **29**, 210 (2014);
    https://doi.org/10.1089/cbr.2014.1614
18. L. Wang, C. Li, Q. Lin, X. Zhang, H. Pan, L. Xu, Z. Shi, D. Ouyang and X. He, *Acta Biochim. Biophys. Sin.*, **47**, 459 (2015);
    https://doi.org/10.1093/abbs/gmv030
19. A.J. Huh and Y.J. Kwon, *J. Control. Rel.*, **156**, 128 (2011);
    https://doi.org/10.1016/j.jconrel.2011.07.002
20. S. Pal, Y.K. Tak and J.M. Song, *Appl. Environ. Microbiol.*, **73**, 1712 (2007);
    https://doi.org/10.1128/AEM.02218-06
21. S. Prabhu and E.K. Poulose, *Int. Nano Lett.*, **2**, 32 (2012);
    https://doi.org/10.1186/2228-5326-2-32
22. K.S. Lee and M.A. El-Sayed, *J. Phys. Chem. B*, **110**, 19220 (2006);
    https://doi.org/10.1021/jp062536y

23. M.S. Abd El-Lat, D.A. Yousif, N.A. Ahmed, G.R. Abd Allah, Y.A. Elbagoury, N.E. El Sayed, H.A. Hassan, B.M. El-hefnawy, A.R. Nageh, E.-S.S. Amer, A.H. Mohamed, N.A. Gobba and M.A. Hussein, *Pak. J. Nutr.*, **20**, 37 (2021);
https://doi.org/10.3923/pjn.2021.37.45

24. A. H. Mohamed, M.A. K. Ibrahem, A. A. Elgazar, H. M. Shabib, E. A. Morsy, S. A. Salah, Y. H. Ibrahem, D. M. Mohamed, N. A. Gobba, M. A. Salem, F. M. Ahmed, A. A. Ali and M. A. Hussein, *Pak. J. Nutr.*, **20**, 9 (2021);
https://doi.org/10.3923/pjn.2021.9.17

25. M.A. Hussein, H.A. El-gizawy, N.A. Gobba and Y.O. Mosaad, *Curr. Pharm. Biotechnol.*, **18**, 677 (2017);
https://doi.org/10.2174/1389201018666171004144615

26. D. Mahor, V. Kumari, K. Vashisht, R. Galgalekar, R.M. Samarth, P.K. Mishra, N. Banerjee, R. Dixit, R. Saluja, S. De and K.C. Pandey, *BMC Pulm. Med.*, **20**, 302 (2020);
https://doi.org/10.1186/s12890-020-01323-3

27. S.R. Kim, H.S. Seo, H.S. Choi, S.G. Cho, Y.K. Kim, E.H. Hong, Y.C. Shin and S.G. Ko, *Evid. Based Complement. Alternat. Med.*, **2013**, 5350 (2013);
https://doi.org/10.1155/2013/975350

28. S. Kamaraj, P. Anandakumar, S. Jagan, G. Ramakrishnan and T. Devaki, *Eur. J. Pharmacol.*, **649**, 320 (2010);
https://doi.org/10.1016/j.ejphar.2010.09.017

29. J. Bartalis and F.T. Halaweish, *J. Chromatogr. B Analyt. Technol. Biomed. Life Sci.*, **818**, 159 (2005);
https://doi.org/10.1016/j.jchromb.2004.12.020

30. S. Tommasi, A. Zheng, J.I. Yoon and A. Besaratinia, *Carcinogenesis*, **35**, 1726 (2014);
https://doi.org/10.1093/carcin/bgu026

31. T. Shimada and Y. Fujii-Kuriyama, *Cancer Sci.*, **95**, 1 (2004);
https://doi.org/10.1111/j.1349-7006.2004.tb03162.x

32. G. Bergers, R. Brekken, G. McMahon, T.H. Vu, T. Itoh, K. Tamaki, K. Tanzawa, P. Thorpe, S. Itohara, Z. Werb and D. Hanahan, *Nat. Cell Biol.*, **2**, 737 (2000);
https://doi.org/10.1038/35036374

33. C.F. Chantrain, H. Shimada, S. Jodele, S. Groshen, W. Ye, D.R. Shalinsky, Z. Werb, L.M. Coussens and Y.A. DeClerck, *Cancer Res.*, **64**, 1675 (2004);
https://doi.org/10.1158/0008-5472.CAN-03-0160

34. R. Roy, J. Yang and M.A. Moses, *J. Clin. Oncol.*, **27**, 5287 (2009);
https://doi.org/10.1200/JCO.2009.23.5556

35. H.C. Li, D.C. Cao, Y. Liu, Y.F. Hou, J. Wu, J.S. Lu, G.H. Di, G. Liu, F.M. Li, Z.L. Ou, C. Jie, Z.Z. Shen and Z.M. Shao, *Breast Cancer Res. Treat.*, **88**, 75 (2004);
https://doi.org/10.1007/s10549-004-1200-8

36. D. Majumder, R. Debnath and D. Maiti, *Life Sci.*, **260**, 118384 (2020);
https://doi.org/10.1016/j.lfs.2020.118384

37. J. Briede, M. Stivrìòa, D. Stoldere, E. Bisenieks, J. Uldriíís, J. Poikâns, N. Makarova and G. Duburs, *Cell Biochem. Funct.*, **22**, 219 (2004);
https://doi.org/10.1002/cbf.1091

38. H.A. El Gizawy, H.M. Abo-Salem, A.A. Ali and M.A. Hussein, *ACS Omega*, **6**, 20492 (2021);
https://doi.org/10.1021/acsomega.1c02340

39. M.R. Shehata, M.M. Mohamed, M.M. Shoukry, M.A. Hussein and F.M. Hussein, *J. Coord. Chem.*, **68**, 1101 (2015);
https://doi.org/10.1080/00958972.2015.1007962

40. M.M. Ghorab, Z.H. Ismail and M. Abdalla, *Arzneimittel-Forschung/Drug Res.*, **60**, 87 (2010);
https://doi.org/10.1055/s-0031-1296254

41. M.A. Hussein, *J. Med. Food*, **21**, 246 (2013);
https://doi.org/10.1089/jmf.2012.0183